

# Plasma Waves in the Magnetotail of Uranus

W. S. KURTH AND D. A. GURNETT

*Department of Physics and Astronomy, University of Iowa, Iowa City*

F. L. SCARF<sup>1</sup>

*TRW Space and Technology Group, Redondo Beach, California*

B. H. MAUK

*Applied Physics Laboratory, Johns Hopkins University, Laurel, Maryland*

As the Voyager 2 spacecraft left Uranus during its encounter with the planet on January 24, 1986, it passed through the magnetotail over the distance range of about  $11 R_U$  to  $79 R_U$ . During this interval the plasma wave receiver on board measured only very weak plasma wave intensities. The most remarkable of these waves are found predominantly inside of about  $23 R_U$  with an additional event occurring between about 48 and  $56 R_U$ . The frequency of these magnetotail plasma waves is generally below about 100 Hz, extending down to the 10-Hz lower frequency limit of the receiver. In each case the upper frequency limit of the emissions lies below the local electron cyclotron frequency. The plasma waves are found prior to the first neutral sheet crossing and between the second and third neutral sheet crossings, as defined by the Voyager magnetometer investigation. This timing suggests the waves are found only in the negative solar magnetospheric lobe of the tail, corresponding to field lines which intersect the planet near the southern magnetic pole—that which is continuously in the nightside hemisphere during the encounter epoch. The observations are not conclusive as to the mode of propagation of the waves. However, the spectrum is similar in some respects to broadband electrostatic waves observed in similar regions of Earth's magnetotail.

## 1. INTRODUCTION

The Voyager 2 encounter of Uranus provided a trajectory which carried the spacecraft through the nightside magnetosphere and down a well-developed magnetotail [Ness *et al.*, 1986]. The encounter provided an opportunity to observe plasma wave phenomena in a variety of regions within the magnetotail, and here we describe those observations.

The Uranian magnetotail represents an interesting magnetospheric structure in view of the (current) nearly sunward alignment of the rotational axis of the planet and the extraordinary  $60^\circ$  tilt of the magnetic dipole with respect to the mechanical axis. The observations of magnetic fields, plasma, and energetic charged particles within the magnetotail are given by Behannon *et al.* [1987]. Gurnett *et al.* [1986] briefly mentioned the existence of weak, low-frequency plasma waves in the near magnetotail of Uranus; however, there was no discussion of the nature of these waves or the implications the waves might have for the physics of the magnetotail. Based on extended studies of the terrestrial magnetotail, one would expect plasma waves to be a prominent constituent of the magnetotails of other planets.

Behannon *et al.* [1987] stress the similarities between the Uranian tail and the terrestrial case. The primary pressure in the tail plasma sheet is caused by protons and electrons with energies below about 6 keV. Protons with energy greater than about 28 keV contribute less than 5% of the plasma sheet

pressure. Behannon *et al.* suggest that transients in the tail field and plasma could be the result of substorm activity. The primary evidence for this is in the low-energy charged particles (LECP) data associated with a partial crossing of the neutral sheet near the end of January 25 [Mauk *et al.*, 1987].

The waves observed in the Uranian magnetotail are very weak, generally less than about  $10^{-10} \text{ V}^2 \text{ m}^{-2} \text{ Hz}^{-1}$ . Further, the observed waves are confined to three general regions traversed after leaving the high-radiation region near the planet. The first region corresponds quite well with the so-called "horns" of the plasma sheet and is not in the magnetotail proper, although the connection with magnetotail physics is obvious. The other two regions correspond to the plasma sheet boundary layer and either the magnetopause boundary layer or the lobe. In each case the regions are associated with the southern magnetic pole, that is, the pole in the darkside hemisphere during the Voyager encounter epoch. Energetic ions ( $> 28 \text{ keV}$ ) show evidence of field-aligned streaming in these regions [Mauk *et al.*, 1987]; however, there is little detailed correlation between the waves and specific field-aligned particle distributions. Neither is there an obvious correlation of the wave activity with flowing plasmas observed by the Voyager plasma instrument.

No solid identification of the wave mode is possible in the absence of wave magnetic field observations; however, the spectra are similar in many respects to broadband electrostatic waves observed in regions within the terrestrial magnetotail. It is also possible that some of the waves are whistler mode emissions.

The observations will be presented in section 2, and a discussion of the location of the wave events, their probable mode of propagation, and their association with various plasma and charged particle observations will be given in sec-

<sup>1</sup>Deceased July 17, 1988.

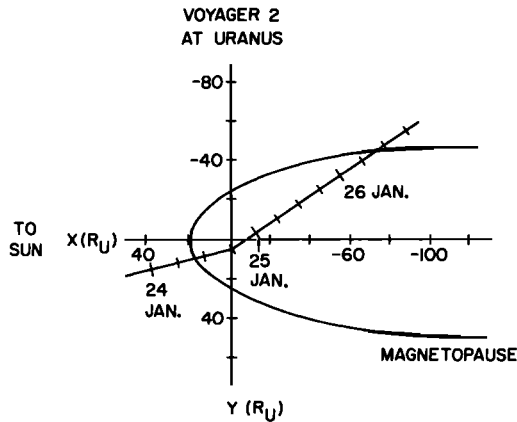


Fig. 1. A sketch of the trajectory of Voyager 2 past Uranus in the plane of the trajectory superimposed on a model magnetopause suggested by *Ness et al.* [1986].

tion 3. The results will be summarized in section 4. No detailed discussion of the instrumentation will be given here, but the information can be found in the review by *Scarf and Gurnett* [1977].

## 2. OBSERVATIONS OF PLASMA WAVES IN THE URANIAN MAGNETOTAIL

The observations presented herein were obtained by the Voyager 2 plasma wave receiver's spectrum analyzer as the spacecraft executed a trajectory, as shown in Figure 1. The trajectory carried the spacecraft in the general downstream (antisunward) direction after the encounter and provided for reasonably good coverage of the magnetotail, given the single-pass character of the flyby.

A summary of the plasma wave observations for the period beginning shortly after the inbound magnetopause crossing until well past the outbound magnetopause crossing is given

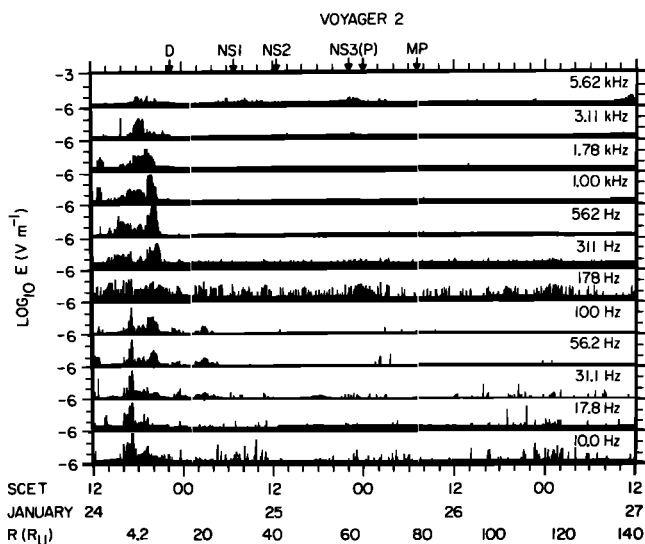


Fig. 2. An overview of the plasma wave observations at Uranus beginning from just inside the inbound magnetopause crossing, through the inner magnetosphere, and out through the magnetotail. The spiky emissions observed at 178 Hz are thought to be instrumental. The D refers to the point where Voyager 2 left the region of intense radiation in the inner magnetosphere. NS1, NS2, and NS3 refer to the three neutral sheet crossings reported by *Ness et al.* [1986], and (P) to a partial neutral sheet crossing. MP refers to the outbound magnetopause crossing.

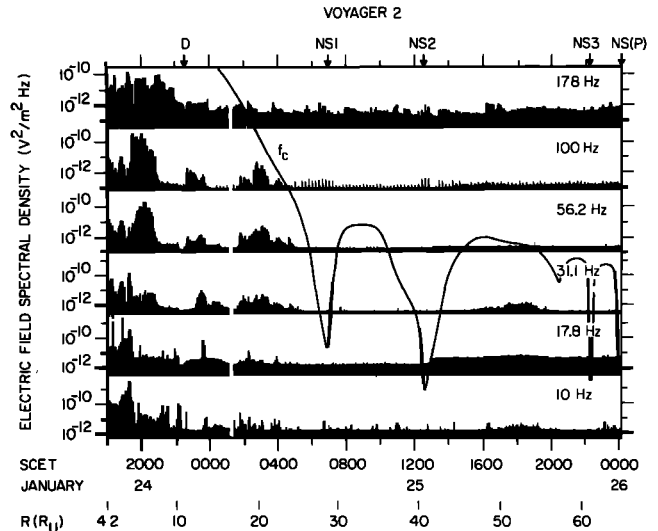


Fig. 3. A closer view of the three intervals of plasma wave activity of interest in this study. The first event begins at the time marked D. The other two events are seen below the  $f_c$  contour just before NS1 and between NS2 and NS3.

in Figure 2. The format of the data is a series of amplitude versus time profiles for each of the 16 spectrum analyzer channels. The magnitude of the electric field averaged over approximately 5-min intervals in each of the channels is indicated by the height of the solid black area above the baseline for the respective channel on a logarithmic scale. The bulk of the wave activity is found within a few hours of closest approach (1800 spacecraft event time (SCET) on January 24) with the most intense of these corresponding to whistler mode waves shortly after closest approach at an intensity of about  $1 \text{ mV m}^{-1}$ . The 178-Hz channel shows relatively intense activity over the entire interval; however, we believe most of the response in this channel to be instrumental in nature. This channel is especially sensitive to impulsive interference such as that from the LECP stepper motor and attitude control thruster activity. While the mechanism for the interference is not understood, such impulses appear to resonate at a frequency within the 178-Hz channel's passband, thereby causing an enhanced response in the channel. We will generally ignore activity in the 178-Hz channel. The most striking observation from Figure 2 is the very weak wave levels observed in the outer magnetosphere and magnetotail, between the times labeled D and MP at the top of the plot. The D corresponds to the sharp decrease in trapped fluxes as the spacecraft left the radiation belts close to the planet [*Mauk et al.*, 1987], and MP refers to the outbound magnetopause crossing [*Ness et al.*, 1986].

There are three regions of wave activity apparent in the lower frequency channels ( $< 178 \text{ Hz}$ ) after about 2200 SCET on January 24. There are centered near 2300 on January 24 and 0300 and 1800 SCET on January 25. Figure 3 shows these three intervals of wave activity in greater detail. Figure 3 is in a format similar to that of Figure 2 but with only the lower six frequency channels shown for greater amplitude resolution and with about 2-min averaging intervals. Superimposed on the data is a curve representing the electron cyclotron frequency  $f_c = 28|B|$ , where  $f_c$  is in hertz and  $|B|$  is in nanoteslas taken from *Ness et al.* [1986]. Note that all three wave events are confined to frequencies below  $f_c$ .

The first wave event of interest in Figure 3 begins almost

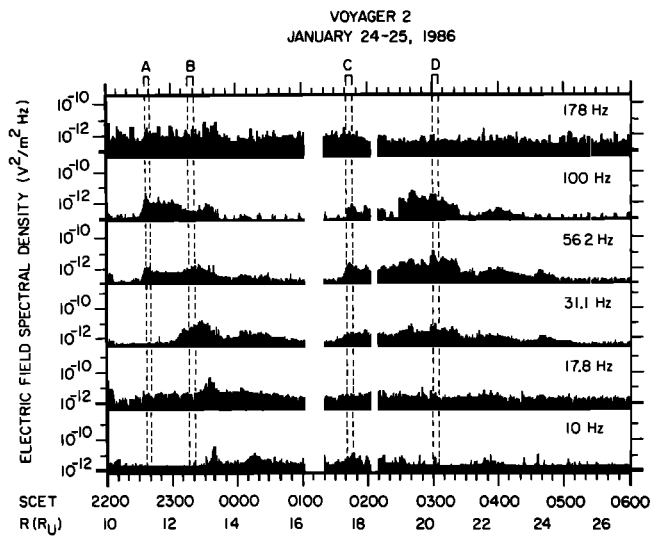


Fig. 4. An expanded plot showing the first two events and their evolution in time. The four intervals marked A–D refer to spectra shown in Figures 5 and 6.

exactly at the time marked D on the top of the figure and has a duration of a little more than an hour at 100 Hz and nearly 2 hours at 17.8 Hz. The second event begins first at lower frequencies at about 0140 SCET on January 25 and lasts until about 0500 SCET at 56.2 Hz. The final event of interest here can be seen at 10 Hz and 31.1 Hz between about 1600 and 2000 SCET, although there is also evidence of this event at 17.8 and 56.2 Hz. Note that the abrupt onset of 17.8-Hz noise at about 1300 corresponds to a change in the data mode on the spacecraft and is thought to be interference associated with the planetary radio astronomy instrument. This interference has the effect of masking the event near 1800 SCET at 17.8 Hz.

The first two events in Figure 3 occur before the first neu-

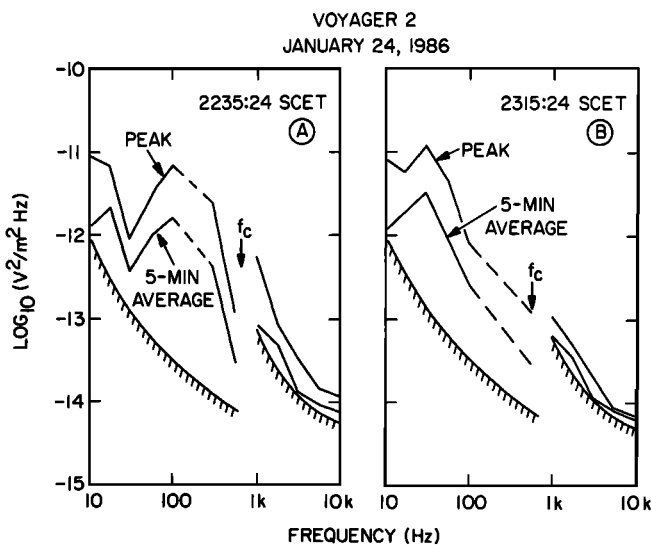


Fig. 5. Spectra obtained during two time periods within the first plasma wave event marked A and B in Figure 4. The spectra are obtained over a 5-min interval during which the average field strength is calculated and the maximum intensity at each frequency is determined to produce the average and peak spectra. The dashed lines indicate our reluctance to interpret noise in the frequency range of a couple of hundred hertz because of spacecraft interference. The hatched lines represent the receiver threshold.

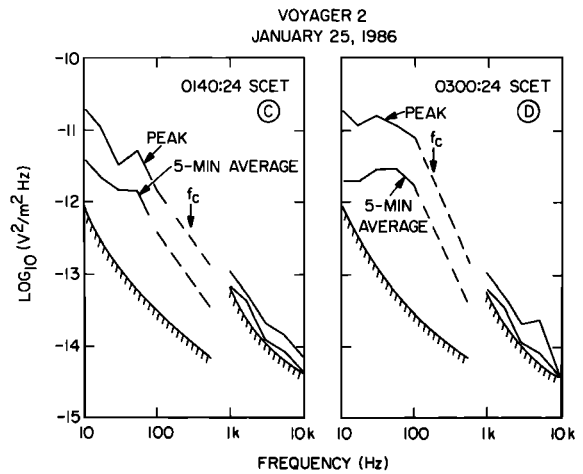


Fig. 6. Same as Figure 5 except that these two sets of spectra are taken from the second interval of wave activity.

tral sheet crossing (NS1) in the magnetotail [Ness *et al.*, 1986] indicated by the dramatic decrease in  $|B|$ , hence  $f_c$ . The third event lies between the second and third neutral sheet crossings (NS2 and NS3) as determined by the Voyager magnetometer. Interestingly enough, there is no evidence for emissions in this frequency range in the opposite tail lobe, that is, between the first and second sheet crossings. The locations of these events will be discussed further in section 3.

As can be seen in Figure 3, the temporal and spectral behavior of the first two events is not simple. The third event shows a simple rise and fall in intensity in each of the channels at about the same time. The first two events, however, show peaks at different frequencies at different times. This effect is further illustrated by the use of a higher temporal resolution display of the first two events in Figure 4 and amplitude versus frequency spectra taken at various times given in Figure 5 and 6.

Figure 4 uses 36-s averages to show the temporal evolution of the spectra of the two wave events observed prior to the first neutral sheet crossing. The first event tends to drift to lower frequencies with increasing time, while the second event shows the opposite effect. The term “drift” really is inaccurate, however, upon close inspection of Figure 4. In the case of the event beginning about 2230 SCET, it would be more accurate to say that the event is confined to the 56.2- and 100-Hz channels (possible extending to 178 Hz) prior to 2300 and is followed by an emission which extended to lower frequencies between 2300 and 0000 SCET on January 25. Finally, after 0000 SCET, the higher frequency emission has all but disappeared, while there is significant activity down to the 10-Hz limit of the receiver. It would be reasonable to suggest that more than one wave mode is responsible for these observations.

The two panels in Figure 5 show peak and 5-min average spectra from the first interval of wave activity taken at times designated A and B in Figure 4. Spectra in panel A taken beginning at 2235:24 SCET show a pronounced peak at 100 Hz and perhaps above. The dashed lines between 100 and 562 Hz indicate our reluctance to interpret bursty activity near 178 Hz as a real signal because of the impulsive interference typically present in this channel. A second component is apparent in the 10- and 17.8-Hz channels. The most intense emissions have an electric field spectral density of  $10^{-11} \text{ V}^2$

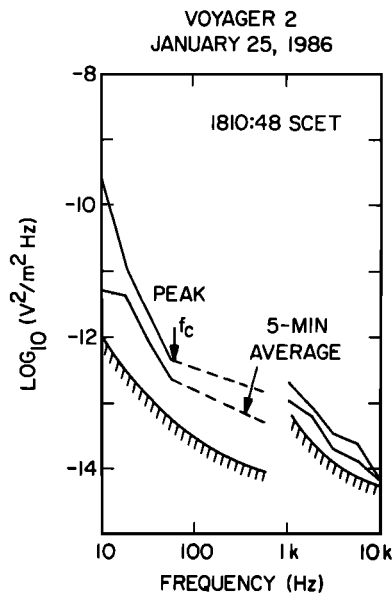


Fig. 7. A peak and average spectrum obtained from the third interval of wave activity seen in Figure 3. Note that the peak in the spectrum appears to be below the 10-Hz lower frequency limit of the instrument.

$m^{-2} Hz^{-1}$ . Spectra shown in Figure 5b are simpler; they show a single peak near 30 Hz with an amplitude similar to that in Figure 5a. For both Figures 5a and 5b the cyclotron frequency bounds the spectral features on the high-frequency side. The hatched lines below the spectra indicate the threshold of the receiver; the mismatch at 1 kHz is due to the calibration uncertainty caused by a failure in the spacecraft's data system.

Figure 6 shows spectra from two times marked C and D during the second interval in Figure 4. Both sets of spectra show a peak near 50 Hz, although this peak is broader in panel D. Again the spectral features appear to be loosely bounded on the upper side by the cyclotron frequency. The maximum amplitudes are about  $2 \times 10^{-11} V^2 m^{-2} Hz^{-1}$ , similar to those in the earlier event.

Figure 7 shows the simple spectral form of the third event, near 1810 SCET on January 25. The peak of this event is at or below the 10-Hz lower frequency limit of the instrument, and the amplitude falls in monotone fashion with increasing frequency. Here the maximum electric field spectral density is  $3 \times 10^{-10} V^2 m^{-2} Hz^{-1}$ , corresponding to about  $25 \mu V m^{-1}$ . The upper frequency limit of the event coincides quite closely with the local electron cyclotron frequency as determined by the magnetometer.

### 3. DISCUSSION

The wave activity observed in the Uranian magnetotail is very weak and confined to three quite well defined events. The spectral extent of each event is limited to less than the local cyclotron frequency. Since the observations of these waves are limited to those presented in the previous section, we turn to other sources of information for clues as to the origin of the waves.

#### 3.1. Location of Wave Events

As pointed out above, the wave activity seems to be ordered in some sense by the neutral sheet crossings. To pursue this issue further, we turn to a presentation of the Voyager 2 tra-

jectory on the nightside of Uranus in a solar-magnetospheric meridian plane projection taken from *Mauk et al.* [1987] shown in Figure 8. The hatched region represents the plasma sheet, and the dashed lines represent dipole magnetic field lines. The construction is very similar to one given by *Bridge et al.* [1986] as an interpretation of the plasma observations. The Voyager trajectory in Figure 8 is highlighted during the intervals of wave activity; the segment highlighted closest to the planet corresponds to the intense whistler mode emissions seen within the higher density regions associated with the inner magnetosphere.

Figure 8 immediately suggests that the first interval of wave activity studied herein (centered near 2300 SCET on January 24) corresponds very closely to the "horn" of the plasma sheet. This is similar to the region where *Gurnett and Frank* [1977] report intense broadband electrostatic wave activity in the terrestrial magnetosphere. In the high-latitude extension of the plasma sheet boundary layer one would expect to find particles streaming along field lines, having been scattered in pitch angle by some currently unknown process.

The second event, from near 0300 on January 25, is located near the lower edge of the plasma sheet, as sketched in Figure 8. This position suggests a relationship with a possible plasma sheet boundary layer, a region where at Earth one often sees intense broadband emissions associated with plasmas streaming along the field lines [*Gurnett et al.*, 1976]. There is a definite gap between the end of this second event and the first neutral sheet crossing, which one would expect to find deeply embedded in the plasma sheet. This position with respect to the neutral sheet suggests the waves are associated not with the heart of the plasma sheet, but with the boundary layer.

The third event is located as far from the plasma sheet as possible after the second neutral sheet crossing and suggests a lobe location for these waves. The large distance from the model plasma sheet discourages any notion of a plasma sheet boundary layer source for the waves in the third event, however, *Mauk et al.* [1987] report evidence of temporal vari-

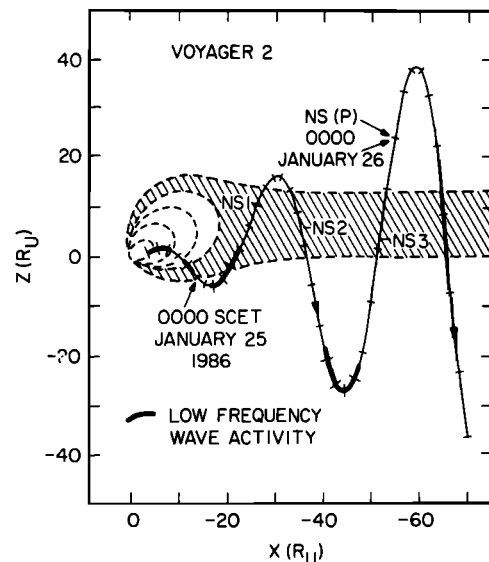


Fig. 8. A construction based on that of *Mauk et al.* [1987], showing the occurrence of plasma wave activity as a function of position with respect to an assumed stable plasma sheet. The first interval of enhanced wave activity on this plot corresponds to the very intense whistler mode waves observed in the inner magnetosphere and is not the subject of this paper.

ations possibly consistent with substorm activity. Another possibility is that the third event is actually associated with the magnetopause boundary layer, since the spacecraft is relatively near the magnetopause (F. V. Coroniti, personal communication, 1988). This suggestion is also consistent with an interpretation of broadband electrostatic waves for the emissions; Scarf *et al.* [1984] report observations of the electrostatic waves in the terrestrial magnetopause boundary layer.

A striking observation from Figure 8 is that all of the wave activity discussed herein occurs in the negative  $Z$  hemisphere, corresponding to field lines which have their feet in the southern magnetic pole which, in the current epoch, is always on the nightside. One explanation for the north-south asymmetry is that the trajectory favors the negative hemisphere; hence there is less likelihood of observing the low-frequency waves in the positive hemisphere. On the other hand, based on the analysis of the field and plasma during the tail trajectory by Behannon *et al.* [1987], the interval between the first and second neutral sheet crossings appears to be a good one for observing boundary layer plasmas and associated waves, similar to the wave event observed just prior to the first neutral sheet crossing. Also there is ample sampling of the northern lobe after the third sheet crossing; however, the partial crossing (NS(P)) occurred in this interval, and it is not clear where the lobe is actually traversed.

Another possibility for the asymmetric occurrence of plasma waves in the southern hemisphere is the asymmetry caused by the large offset and tilt in the magnetic dipole. The southern magnetic pole is always on the nightside during the current epoch, and the surface field strength is greatest in this hemisphere. Other asymmetries have been reported, most notably the north-south (day-night) asymmetry in radio emissions from the planet [Warwick *et al.*, 1986]. Radio emissions emanating from the dayside hemisphere (northern magnetic pole) are very weak as compared to those observed coming from the nightside hemisphere (see, for example, Gulkis and Carr [1987], Leblanc *et al.* [1987], Lecacheux and Ortega-Molina [1987], Romig *et al.* [1987], and Zarka and Lecacheux [1987]). Broadfoot *et al.* [1986] report prominent auroral emissions on the nightside, but electroglow dominates the dayside. Since intense radio emissions are often associated with auroral field lines and electron distributions on those field lines set up by the precipitation of energetic particles, it is conceivable that distributions farther down the tail on those same field lines are asymmetric with respect to those connecting to the dayside hemisphere and may be more conducive to instabilities which would drive plasma waves. We will look at particle observations below which might bear on this question also.

The observations of wave activity in the Uranian tail can be compared to terrestrial observations. As a first comparison the spectral densities reported above are 2–3 orders of magnitude weaker than those of broadband electrostatic noise reported in the terrestrial tail at distances of 34–217  $R_E$  by Scarf *et al.* [1984]. Scarf *et al.* [1974, 1977] report electromagnetic waves below  $f_c$  in the terrestrial plasma sheet and in the magnetopause boundary layer. Scarf *et al.* conclude that these were whistler mode waves. The apparent confinement below  $f_c$  of the Uranian waves presented here is consistent with the whistler mode. Other waves reported in Earth's distant tail include electron plasma oscillations and continuum radiation [Coroniti *et al.*, 1984], but these are higher frequency waves

occurring at or above  $f_p$  and almost certainly do not correspond to the waves in the Uranian tail. (A discussion of the likely value of  $f_p$  in the tail is found below.) The location of broadband electrostatic noise observed at Earth is a very interesting factor to be compared with the Uranian observations. Gurnett and Frank [1977] report the high-latitude extension of the plasma sheet boundary layer is very often the site of intense broadband electrostatic turbulence. This location is very similar to the location of the first event reported herein centered on about 2300 SCET on January 24. As described above, the first event was located very close to the so-called "horns" of the plasma sheet and therefore is consistent with the location reported by Gurnett and Frank at Earth. Further, Gurnett *et al.* [1976] report that in the more distant terrestrial magnetotail (near 40  $R_E$ ) the outer boundary of the plasma sheet is a favored location for the existence of broadband electrostatic noise. Observations deeper in the tail from ISEE 3 [Scarf *et al.*, 1984] support both the plasma sheet and magnetopause boundary layers as locations of the broadband noise. Scarf *et al.* also discuss the observations of a broadband electrostatic mode, perhaps Doppler-shifted ion-acoustic waves, located above  $f_c$  in the boundary layer. This latter observation appears to be precluded at Uranus on the basis of its frequency lying above  $f_c$ .

The location of the third event with respect to the plasma sheet and magnetopause is not well established. As Mauk *et al.* [1987] state, the Uranian tail seems to display very dynamic behavior, and the distance from the plasma sheet or magnetopause to the spacecraft during the third event is not known with any degree of reliability. Either site, however, would be consistent with the location of terrestrial broadband electrostatic noise. A deep lobe location would not be as compatible with the terrestrial case, though [Gurnett *et al.*, 1976].

### 3.2. Wave Mode

We have not yet discussed the possible mode of propagation of the waves observed in the Uranian magnetotail. While we will suggest one or two possibilities in this section, it should be clear from the outset that insufficient information is available to unambiguously determine the mode. The information which is available includes the spectra and amplitudes given in section 2 along with information on the cyclotron frequency shown in Figure 3. Another critical piece of information in determining the wave mode is the position of the wave spectrum with respect to the electron plasma frequency  $f_p$ .

There is little information of use in the plasma wave spectrum to determine  $f_p$ . The existence of bursty electromagnetic emissions in the frequency range of a few kilohertz [Kurth *et al.*, 1986] offers an upper limit of  $0.1 \text{ cm}^{-3}$  for  $f_p$ , since the electromagnetic emissions could not propagate through the tail to the spacecraft if the intervening plasma frequency were equal to or greater than the wave frequency. Sittler *et al.* [1987] give an estimate based on <6-keV electrons of about  $10^{-3} \text{ cm}^{-3}$  in the lobes. Behannon *et al.* [1987] deduce an average lobe plasma density of  $1.7 \times 10^{-3} \text{ cm}^{-3}$  by using the pitch angle of a helical field in a plasma. The observed pitch angle of the field was about  $5.5^\circ$ . Since the plasma frequency corresponding to  $10^{-3} \text{ cm}^{-3}$  is about 285 Hz and this is well above the upper frequency cutoff of the waves discussed herein (with the exception of the first event), it is probably safe to assume that the waves observed in the tail lie below  $f_p$ . In fact, for the one event most likely to be in the lobe near 1800 SCET on January 25 the plasma density could be as low as about

$3 \times 10^{-5} \text{ cm}^{-3}$  without being of consequence in this discussion, since the waves would still lie below  $f_p$ .

The Voyager instrumentation does not include a magnetic sensor with sensitivity above about 8 Hz; hence there is no way to know whether the waves observed are electrostatic or electromagnetic. The existence of enhanced magnetic field fluctuations below 8 Hz (where the magnetometer is sensitive to fluctuating magnetic fields) would be consistent with electromagnetic radiation if one assumes the electric field spectrum extends to frequencies as low as the magnetic fluctuations. However, inspection of the root mean square magnetic field deviations published by *Ness et al.* [1986] for the appropriate times reveals little, if any, evidence for magnetic fluctuations below 8 Hz. Voyager does not provide a method of determining polarization at these low frequencies, since the spacecraft did not rotate at times appropriate for looking for spin modulation.

Based on the meager information available and analogies with observations at Earth, we offer two possible suggestions for the mode of propagation of the waves observed in the Uranian magnetotail. First, the fact that the waves occur below  $f_c$  and probably below  $f_p$  is consistent with the waves being in the whistler mode, which lies below the lower of these two critical frequencies. Unless the magnetic signature of the emissions can be ruled out in some way, the whistler mode must be retained as a possibility. This mode would be consistent with the *Scarf et al.* [1974, 1977] observations of whistler mode waves in the plasma sheet and magnetopause boundary layer at Earth.

The second suggestion for an identification of the waves is prompted by the spectra in Figures 5–7, which are broadband and peak near the lowest frequencies measured as well as being located near the high-latitude extension of the plasma sheet (the first event), the plasma sheet boundary layer (the second event), or perhaps the magnetopause boundary layer (third event). These attributes are very reminiscent of broadband electrostatic noise [*Gurnett et al.*, 1976; *Gurnett and Frank*, 1977; *Scarf et al.*, 1984]. At Earth, broadband electrostatic noise is sometimes known to extend up to the electron plasma frequency in regimes where  $f_c < f_p$  (although the spectra presented by *Gurnett and Frank* [1977] seem to show a cutoff below  $f_c$ ). The uncertainty in  $f_p$  makes it difficult to confirm this characteristic at Uranus. For the event late in the day of January 25 the plasma density would have to be nearly 2 orders of magnitude smaller than the *Behannon et al.* [1987] and *Sittler et al.* [1987] estimates. It is also possible, in view of the weak appearance of the waves, that the high-frequency portion of the wave spectrum is simply below detection with the short (7 m) dipole antenna utilized on Voyager. A comparison of the spectra shown in Figures 5 and 6 with those given by *Gurnett and Frank* [1977] for broadband electrostatic noise reveals similarities in that both Uranian and terrestrial spectra are likely to be complex, with peaks appearing on an otherwise monotone decreasing trend.

Given the general similarities in spectral form and location within the magnetotail, we believe the Uranian waves are most similar to the terrestrial broadband electrostatic noise.

### 3.3. Association With Charged Particle Observations

The presence of locally generated plasma waves implies the existence of unstable distributions of plasma to drive the waves. It is natural, then, to examine the plasma observations

for evidence of plasma distributions which might be responsible for the waves observed in the Uranian magnetotail. Our search for evidence of unstable plasmas is focused by the tentative wave identification made above. Considerable progress at Earth has been made in correlating the observations of field-aligned ion beams or counterstreaming ion beams with the occurrence of broadband electrostatic noise in the geotail (see, for example, *Gurnett et al.* [1976], *Grabbe and Eastman* [1984], *Omidi* [1985], *Dusenbery and Lyons* [1985], *Ashour-Abdalla and Okuda* [1986], and *Akimoto and Omidi* [1986]).

The limited instrumentation on board Voyager makes analyses of particle distributions difficult. While the plasma instrument (PLS) has four detectors mounted in a configuration so as to provide some information on the shape of the distribution [*Bridge et al.*, 1977], the task is highly model dependent, and the sensors have fairly broad apertures; detection of plasma streaming would be possible but dependent on the direction of flow. Similarly, the LECP instrument is designed to mechanically step the direction of its sensors so as to provide pitch angle coverage, but typical stepping rates (often minimized in order to reduce the impact of interference on instruments such as the plasma wave receiver) are slow enough to be of little use on transient events. Nevertheless, some observations have been reported which are consistent with the type of particle flows which might be expected to accompany broadband electrostatic noise.

*Mauk et al.* [1987] have reported the detection of field-aligned flows of protons in the energy range 28–43 keV, particularly in regions near the plasma sheet boundary layer. In fact, a comparison of Figure 8 with Figure 17 of *Mauk et al.* leads to an initial impression that there is a reasonably good correspondence between some of the regions showing planetward streaming and the plasma wave activity discussed herein. Considerable streaming seems to be present during the second plasma wave event (near 0300 SCET on January 25). *Mauk et al.* also point out planetward streaming near the end of the third wave event.

A more detailed view of the comparison between proton streaming and wave activity is given in Figure 9, where a superposition of the LECP flow data with the plasma wave spectrum information is provided. At the top of the figure the vectors indicate the two-dimensional direction and relative speed of plasma streaming as a function of time. The small construction in the upper left corner shows the directions for sunward (S) and planetward (U) streaming. The count rate profiles in the upper panel provide a measure of the intensity of the flows based on the number of particles detected at the time. The dotted vectors indicate determinations limited by low count rates.

As can be seen in Figure 9, the detailed comparison of the streaming observations with the plasma wave activity does not present a strong sense of correlation. There are tailward flows toward the end of the first event, but only after the flux has dropped considerably. The latter portion of the event centered on 0300 SCET on January 25 correlates reasonably well with planetward flows and substantial count rates. The rates at this time are smaller than but comparable to the fluxes observed within the plasma sheet itself. The count rates during the third wave event are sufficiently low to preclude solid conclusions about streaming, but toward the end of the event, fluxes rise, and a significant planetward flow is again observed. Other intervals of streaming are observed, however, with no resulting wave activity; hence it is difficult to make a very convincing

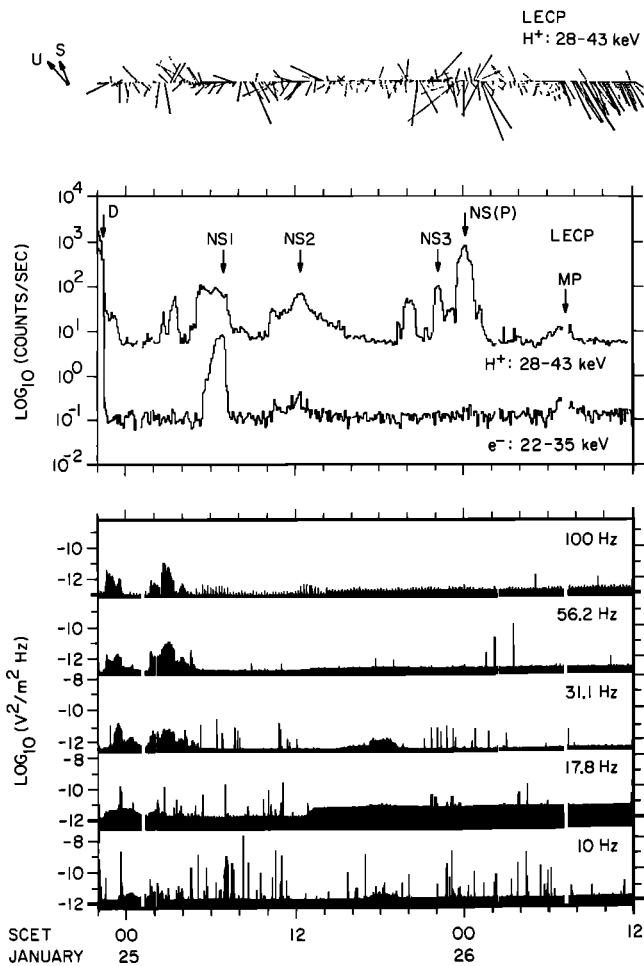


Fig. 9. A comparison of ion streaming measurements from the LECP instrument and regions of plasma wave activity observed by the plasma wave instrument. While there is general correspondence between the wave activity and field-aligned flows, the correlation is not impressive in detail.

argument on the relationship of the wave activity and streaming ions. It must be noted, however, that theory dictates that the presence of a beam alone is not sufficient to drive the instability. If the beam is warm, then an additional cold beam must be present in the plasma to drive it unstable [e.g., *Dusenberry and Lyons, 1985*].

*Behannon et al.* [1987] report on the importance of <6-keV ions in the overall pressure balance in the tail at Uranus and concludes that they make a significant contribution in the plasma sheet. Unfortunately, interference effects precluded observations of the low-energy ions beyond the plasma sheet, so it is not possible to establish the existence of a correlation between these ions and the wave activity.

#### 4. SUMMARY

The Voyager 2 plasma wave receiver detected the presence of weak, broadband waves in the high magnetic latitude extensions of the tail plasma sheet, near the plasma sheet boundary layer, and in the tail lobe at Uranus. In each case the spacecraft was on field lines whose feet were in the southern or nightside magnetic hemisphere. The spectrum of the wave activity was sometimes simple and monotone, decreasing with increasing frequency but often complicated by low-frequency peaks at one or more frequencies. In all cases the wave activity

was limited to frequencies below the electron cyclotron frequency. While the electron plasma frequency is not well established in the Uranian tail, it is thought that the wave activity is confined to frequencies below  $f_p$  as well.

The shape of the spectrum and the location of the wave activity near the boundary layer suggest that the waves may be similar to broadband electrostatic noise at Earth. The lack of wave magnetic field observations, however, makes it impossible to rule out whistler mode waves. Attempts to correlate the plasma waves with field-aligned ion flows are encouraging but do not show a strong correlation in detail.

Even though the Uranian waves are about a factor of 100 weaker than their terrestrial counterparts, the existence of the emissions suggests similar plasma acceleration processes are occurring in the terrestrial and Uranian magnetotails and that auroral field-aligned plasma flows and related plasma wave phenomena can be found in both magnetotails.

*Acknowledgments.* We are grateful to J. E. P. Connerney of the Voyager magnetometer team for providing magnetic field intensities used in calculating electron cyclotron frequencies. The research at the University of Iowa was supported by NASA through contract 957723 with the Jet Propulsion Laboratory. The research at TRW was supported by NASA through contract 957805 with the Jet Propulsion Laboratory. The effort at APL was supported by NASA under Task I of contract N00039-87-C-5301 between the Johns Hopkins University and the Department of the Navy.

The Editor thanks J. Romig and two other referees for their assistance in evaluating this paper.

#### REFERENCES

- Akimoto, K., and N. Omidi, The generation of broadband electrostatic noise by an ion beam in the magnetotail, *Geophys. Res. Lett.*, **13**, 97, 1986.
- Ashour-Abdalla, M., and H. Okuda, Theory and simulations of broadband electrostatic noise in the geomagnetic tail, *J. Geophys. Res.*, **91**, 6833, 1986.
- Behannon, K. W., R. P. Lepping, E. C. Sittler, Jr., N. F. Ness, B. H. Mauk, S. M. Krimigis, and R. L. McNutt, Jr., The magnetotail of Uranus, *J. Geophys. Res.*, **92**, 15,354, 1987.
- Bridge, H. S., J. W. Belcher, R. J. Butler, A. J. Lazarus, A. M. Mavretic, J. D. Sullivan, G. L. Siscoe, and V. M. Vasyliunas, The plasma experiment on the 1977 Voyager mission, *Space Sci. Rev.*, **21**, 259, 1977.
- Bridge, H. S., et al., Plasma observations near Uranus: Initial results from Voyager 2, *Science*, **233**, 89, 1986.
- Broadfoot, A. L., et al., Ultraviolet spectrometer observations of Uranus, *Science*, **233**, 74, 1986.
- Coroniti, F. V., F. L. Scarf, C. F. Kennel, and D. A. Gurnett, Continuum radiation and electron plasma oscillations in the distant geomagnetic tail, *Geophys. Res. Lett.*, **11**, 661, 1984.
- Dusenberry, P., and L. Lyons, The generation of electrostatic noise in the plasma sheet boundary layer, *J. Geophys. Res.*, **90**, 10,935, 1985.
- Grabbe, C. L., and T. E. Eastman, Generation of broadband electrostatic noise by ion beam instabilities in the magnetotail, *J. Geophys. Res.*, **89**, 3865, 1984.
- Gulkis, S., and T. D. Carr, The main source of radio emission from the magnetosphere of Uranus, *J. Geophys. Res.*, **92**, 15,159, 1987.
- Gurnett, D. A., and L. A. Frank, A region of intense plasma wave turbulence on auroral field lines, *J. Geophys. Res.*, **82**, 1031, 1977.
- Gurnett, D. A., L. A. Frank, and R. P. Lepping, Plasma waves in the distant magnetotail, *J. Geophys. Res.*, **81**, 6059, 1976.
- Gurnett, D. A., W. S. Kurth, F. L. Scarf, and R. L. Poynter, First plasma wave observations at Uranus, *Science*, **233**, 106, 1986.
- Kurth, W. S., D. A. Gurnett, and F. L. Scarf, Sporadic narrow-band radio emissions from Uranus, *J. Geophys. Res.*, **91**, 11,958, 1986.
- Leblanc, Y., M. G. Aubier, A. Ortega-Molina, and A. Lecacheux, Overview of the Uranian radio emissions: Polarization and constraint on source locations, *J. Geophys. Res.*, **92**, 15,125, 1987.
- Lecacheux, A., and A. Ortega-Molina, Polarization and localization of the Uranian radio sources, *J. Geophys. Res.*, **92**, 15,148, 1987.
- Mauk, B. H., S. M. Krimigis, E. P. Keath, A. F. Cheng, T. P. Arm-

- strong, L. J. Lanzerotti, G. Gloeckler, and D. C. Hamilton, The hot plasma and radiation environment of the Uranian magnetosphere, *J. Geophys. Res.*, *92*, 15,283, 1987.
- Ness, N. F., M. H. Acuña, K. W. Behannon, L. F. Burlaga, J. E. P. Connerney, R. P. Lepping, and F. M. Neubauer, Magnetic fields at Uranus, *Science*, *233*, 85, 1986.
- Omidi, N., Broadband electrostatic noise produced by ion beams in the Earth's magnetotail, *J. Geophys. Res.*, *90*, 12,330, 1985.
- Romig, J. H., D. R. Evans, C. B. Sawyer, A. E. Schweitzer, and J. W. Warwick, Models of Uranian continuum radio emission, *J. Geophys. Res.*, *92*, 15,189, 1987.
- Scarf, F. L., and D. A. Gurnett, A plasma wave investigation for the Voyager mission, *Space Sci. Rev.*, *21*, 289, 1977.
- Scarf, F. L., L. A. Frank, K. L. Ackerson, and R. P. Lepping, Plasma wave turbulence at distant crossings of the plasma sheet boundaries and the neutral sheet, *Geophys. Res. Lett.*, *1*, 189, 1974.
- Scarf, F. L., L. A. Frank, and R. P. Lepping, Magnetosphere boundary observations along the IMP 7 orbit, 1, Boundary locations and wave level variations, *J. Geophys. Res.*, *82*, 5171, 1977.
- Scarf, F. L., F. V. Coroniti, C. F. Kennel, R. W. Fredricks, D. A. Gurnett, and E. J. Smith, ISEE 3 wave measurements in the distant geomagnetic tail and boundary layer, *Geophys. Res. Lett.*, *11*, 335, 1984.
- Sittler, E. C., Jr., K. W. Ogilvie, and R. Selesnick, Survey of electrons in the Uranian magnetosphere: Voyager 2 observations, *J. Geophys. Res.*, *92*, 15,263, 1987.
- Warwick, J. W., et al., Voyager 2 radio observations of Uranus, *Science*, *233*, 102, 1986.
- Zarka, P., and A. Lecacheux, Beaming of Uranian nightside kilometer radio emission and inferred source location, *J. Geophys. Res.*, *92*, 15,177, 1987.
- 
- D. A. Gurnett and W. S. Kurth, Department of Physics and Astronomy, University of Iowa, Iowa City, IA 52242.
- B. H. Mauk, Applied Physics Laboratory, Johns Hopkins University, Laurel, MD 20707.

(Received April 11, 1988;  
revised September 15, 1988;  
accepted December 1, 1988.)